Pergamon

Tetrahedron: Asymmetry, Vol. 8, No. 13, pp. 2115–2129, 1997

Printed in Great Britain

PII: S0957-4166(97)00206-1

0957-4166/97 $17.00 + 0.00

Stereogenic competition in bilirubin conformational enantiomerism

Stefan E. Boiadjiev and David A. Lightner *

Department of Chemistry, University of Nevada, Reno, NV 89557-0020, USA

Abstract: Optically active bilirubin analogs (**1** and **2**) with a stereogenic center in each propionic acid side chain were synthesized and examined by CD and NMR spectroscopy. Introduction of an α-methyl and a β-methyl forces the pigment to adopt either a left-handed (***M***) or right-handed (***P***) helicity with a folded, ridge-tile conformation. As evidenced by exciton-type circular dichroism spectra, the (α*S*,α′*S*-**3**), (β*S*,β′*S*-**5**), (α*S*,β′*S*-**1**) stereoisomers strongly prefer the ***M***-helicity ridge-tile conformation, but the (α*R*,β′*S*) stereoisomer (**2**) prefers the ***P***-helicity. © 1997 Elsevier Science Ltd

Introduction

Bilirubin is a hydrophobic metabolite that is poorly excreted and can become toxic if it accumulates in the body. Normally, it does not accumulate to any extent because it is conjugated in the liver to glucuronide metabolites that are less hydrophobic and readily excreted across the liver into bile.[1,2] Optical spectroscopy of bilirubinoid pigments has long been important in the diagnosis of jaundice and in clinical measurements of bile pigments in body tissues. And circular dichroism (CD) spectroscopy has proven to be an excellent technique for elucidating the conformation of the pigment in solution,[3–6] especially in conjunction with NMR measurements.[7]

Bilirubin belongs to the class of pigments called "linear tetrapyrroles"; yet, its solution and biological properties do not correlate well with either the linear structure or a porphyrin-like structure. Its most stable conformation is now known to be bent in the middle, in the shape of a ridge-tile (Figure 1). In the ridge-tile conformation, which is flexible and not rigid, the propionic acid groups are engaged in intramolecular hydrogen bonding to the opposing dipyrrinone lactam and pyrrole components. In bilirubin and its mesobilirubin analogs, where vinyls are replaced by ethyl while retaining propionic acids at C(8) and C(12), considerable conformational stabilization of the ridge-tile shape is achieved through intramolecular hydrogen bonding,[8] leaving the polar groups tucked inward and thus rendering the pigment surprisingly lipophilic.[9]

BILIRUBIN

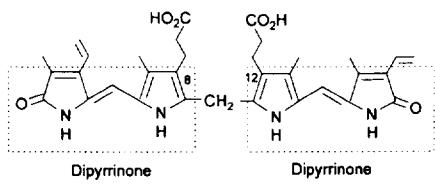

The ridge-tile conformations of Figure 1 with their near-C_2-symmetry are dissymmetric and enantiomeric. In an isotropic medium, bilirubin and its analog mesobilirubin-XIIIα consist of a 50:50 mixture of equilibrating conformational enantiomers. Displacement of the equilibrium toward one or the other of the enantiomers has been achieved by complexation with a chiral compound, such as quinine[6] or serum albumin,[10] and observed by CD of the pigment. Selective stabilization of one enantiomer can also be achieved through intramolecular nonbonded steric interactions, as has been observed when stereogenic centers are created by methyl substitution at either the α or the β carbons of

* Corresponding author. Email: lightner@unr.edu

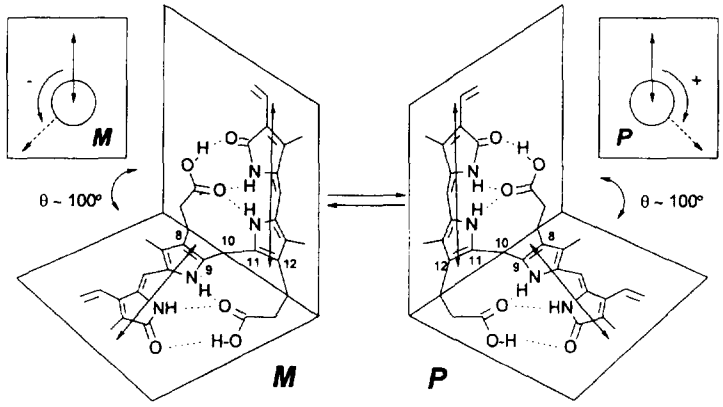

Figure 1. Interconverting intramolecularly hydrogen-bonded enantiomeric conformers of bilirubin-IXα. The double headed arrows represent the dipyrrinone long wavelength electric transition moment vectors (dipoles). The relative helicities (*M*, minus or *P*, plus) of the vectors are shown (inset) for each enantiomer. Dotted lines represent hydrogen bonds.

the propionic acid chains.[5] Such forced "intramolecular resolution" has been achieved in **3** and **5**. The current work focusses on two new diastereomeric analogs (**1** and **2**) that have been designed to probe whether an α-methyl is more effective than a β-methyl in displacing the conformation equilibrium displayed in Figure 1.

MESOBILIRUBIN-XIIIα

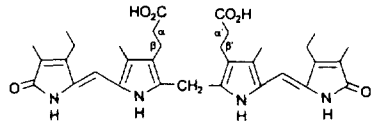

α,β′-DIMETHYLMESOBILIRUBINS-XIII α

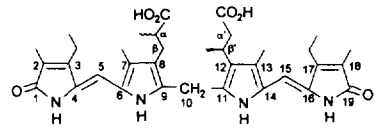

1: α(*S*)CH_3,β′(*S*)CH_3 nonpolar
2: α(*R*)CH_3,β′(*S*)CH_3 polar
3: α(*S*)CH_3,α′(*S*)CH_3 nonpolar
4: α(*R*)CH_3,α′(*S*)CH_3 polar
5: β(*S*)CH_3,β′(*S*)CH_3 nonpolar
6: β(*R*)CH_3,β′(*S*)CH_3 polar

optically active: **1**, **2**, **3**, **5**; optically inactive: **4**, **6**

Results and discussion

Synthesis

Bilirubin analogs **1** and **2** were prepared from known optically active dipyrrinone acid **11**[11] and racemic dipyrrinone ester **10**[5b] as outlined in Scheme 1. Oxidative coupling of an equimolar mixture of **10** and **11** using *p*-chloranil[12] led to a mixture of self-coupled and cross-coupled mesobiliverdin products that were separated by radial chromatography on silica gel. The self-coupled products are enantiomerically pure diacid (β*S*,β′*S*)-**9** and a mixture of dimethyl esters, *rac*-**8** [(α*S*,α′*S*)+(α*R*,α′*R*)] and *meso*-**8** (α*R*,α′*S*). The cross-coupled products, obtained in 81% yield are the diastereomeric mono-esters **7**: (α*S*,β′*S*) and (α*R*,β′*S*). The cross-coupled verdins were saponified then reduced with sodium borohydride to the corresponding rubins, which were separated by radial chromatography and crystallized from chloroform–methanol to give enantiomerically pure **1** and **2**. Other dimethylmesobilirubins (**3**–**6**) of this study are known from earlier work.

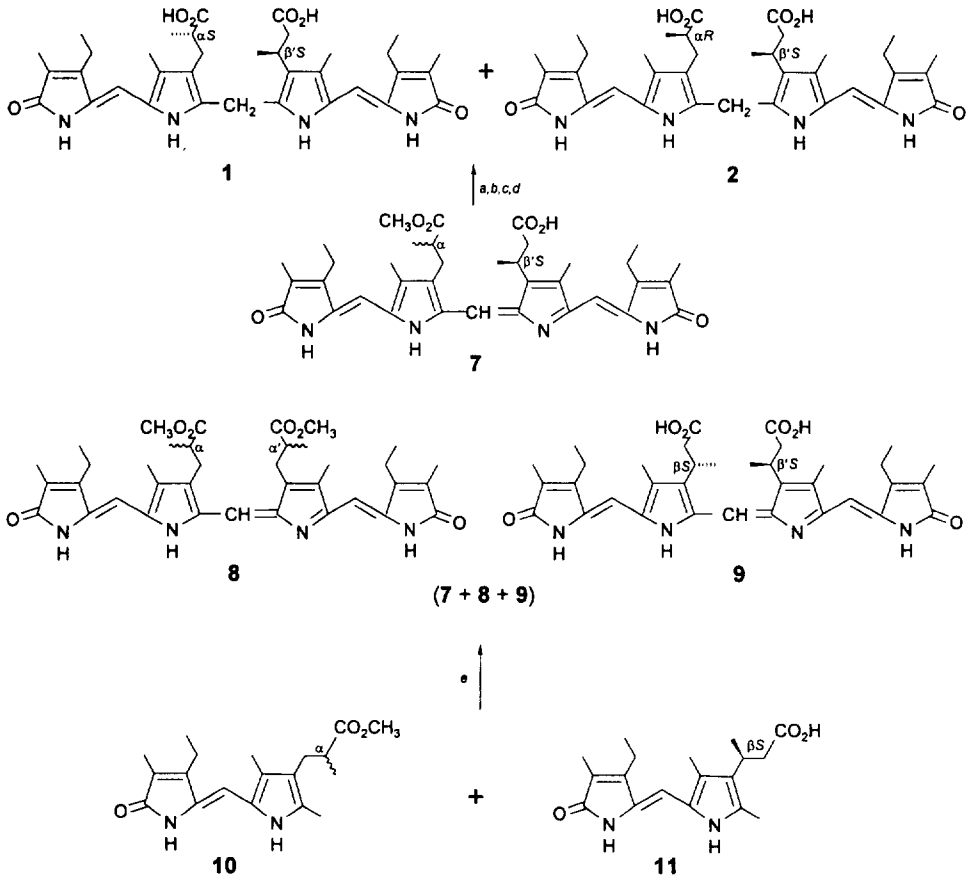

[a] Chromatographic separation of **7** from **8** and **9**. [b] $NaOH/H_2O$, then HCl. [c] $NaBH_4$, CH_3OH, THF then CH_3COOH. [d] Chromatographic separation of **1** and **2**. [e] *p*-chloranil, HCOOH.

Scheme 1. Synthetic scheme.

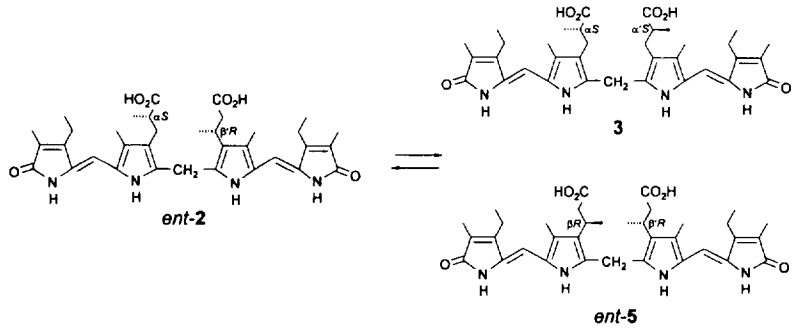

Figure 2. Acid-catalyzed disproportionation of *ent*-**2** using conc. HCl in $(CH_3)_2SO$ to give a mixture of *ent*-**2**, **3** and *ent*-**5**.

Acid-catalyzed constitutional isomerization,[2,12-15] of the enantiomer of **2** (*ent*-**2**), prepared as outlined in the Synthetic Scheme using the enantiomer of **11**, gave a separable mixture of **3**, *ent*-**5** and *ent*-**2** (Figure 2). This links the absolute configuration of the α,α′-dimethylmesobilirubin-XIIIα (**3**), as determined by CD in this work and earlier,[5b] to the β,β′-dimethylmesobilirubins, whose absolute stereochemistry was determined by X-ray crystallography of a monopyrrole synthetic precursor.[5a]

Structure and ^{13}C-NMR spectra

The ^{13}C-NMR spectra of **1** and **2** are compared in Table 1 to those of the isomeric dimethyl rubins **3–6** in $CDCl_3$. As expected, the more symmetric pigments **3** ($\alpha S,\alpha' S$) and **5** ($\beta S,\beta' S$) exhibit the most homogeneous spectra, with no signal doubling. Their *meso* analogs **4** ($\alpha R,\alpha' S$) and **6** ($\beta R,\beta' S$), respectively, exhibit signal doubling for certain carbon resonances. This is consistent with the previously proposed conformational model where one propionic acid group easily hydrogen bonds intramolecularly to an opposing dipyrrinone (Figure 1) but intramolecular hydrogen bonding by the second propionic acid to the remaining dipyrrinone is resisted by non-bonded steric repulsions between an α-CH_3 and a C(7) or C(13) CH_3, or between a β-CH_3 and C(10)-CH_2.[5] This forces a dissymmetry in the ridge-tile, where hydrogen bonding in one half is a snug fit and that of the remaining half is a very loose fit. Thus, for **4** the α-CH_3 resonance at δ 19.66 is thought to correspond to that in the snugly fit half (cf. α-CH_3 of **3**); whereas, the α-CH_3 resonance at δ 19.18 is attributed to that of the loosely fit half.[5,8] Other resonances of **4**, e.g., β-CH_2, C(9)/(11), C(8)/(12), C(4)/(16), correspond nicely. The resonance of the connecting central carbon, C(10), is not doubled, but is deshielded. Similarly, for **6** the β-CH_3 resonance at δ 20.82 is thought to correspond to a snugly fit half (cf. β-CH_3 in **5**), while that at δ 19.74 is thought to correspond to the more loosely fit half. Again, one of the pair in other resonances, e.g., β-CH, α-CH_2, C(9)/(11), C(8)/(12), etc. find good correspondence with those of **5**, where both halves fit snugly, and the resonance of the connecting central carbon, C(10), is not doubled but is deshielded.

In **1** and **2**, where each has one α-CH_3 and one β-CH_3, the ^{13}C-NMR signals are mainly doubled (in **1**) or doubled twice (in **2**). In **1**, where both stereogenic centers have the *S*-configuration, the pigment is expected to adopt the ***M***-helicity ridge-tile (Figure 1). That is, non-bonded steric interactions are minimized in the ***M***-helical conformer but not in the ***P***. Consequently, virtually all of the carbon resonances seen in **1** are also seen in **3** and **5** – as if **1** were a 50:50 mixture of **3** and **5**. The central carbon C(10) is slightly more deshielded in **1** than in **5**, but not as deshielded as in either **4** or **6**. In marked contrast, **2** has two sets of doubled signals, as if both the ridge-tile shapes exhibited the dissymmetry expected in **4** and **6**. In the ***P***-helical conformer of **2**, the propionic acid with the αR-CH_3 would hydrogen bond snugly with its opposing dipyrrinone, but the remaining propionic acid with the $\beta' S$-CH_3 would not. One might thus expect two sets of signals: one set (the ***P***) of ^{13}C-NMR resonances corresponding to those of **4**, and the other set (the ***M***) of resonances corresponding to those of **6** (Table 1). The signals of **P** set are more intense than those of **M** set.

Hydrogen bonding and conformation

In bilirubins, ^1H-NMR chemical shifts of the lactam and pyrrole NH and carboxylic acid OH, and NOEs between NH pairs and between NH and acid OH have been shown to be useful diagnostics for detecting the intramolecular hydrogen bonding that stabilizes the ridge-tile conformations of Figure 1.[5,7,13,16–18] The data of Table 2 indicate very similar OH chemical shifts for **1–6**. The deshielded lactam NH resonances near 10–11 ppm are characteristic of intramolecular hydrogen bonding in bilirubins,[5] as has been shown previously for **3** and **5** and other well-characterized bilirubins. Pyrrole NH resonances near 9 ppm are characteristic of hydrogen bonding in a folded, ridge-tile conformation where the NH of one pyrrole ring lies slightly over (the magnetic anisotropic shielding region of) the other pyrrole ring.[5,7,17,18] In contrast, when two dipyrrinones form a planar dimeric association complex using hydrogen bonds, the pyrrole NH resonance appears at ~10 ppm (and the lactam near 11 ppm).[16–18]

Rubins **3** and **5**, have been shown to adopt preferentially the ***M***-helical conformation (Figure 1).[5] Each exhibit but a single set of NH and OH resonances; the remaining ^1H-NMR signals are not doubled (Table 2). However, doubling of signals occurs in their diastereomers (**4** and **6**) for the same reasons (see above) that their ^{13}C-NMR signals are doubled: although both ***M*** and ***P*** helical conformers are present, only one half of a structure in either case can exhibit a snug fit for hydrogen bonding; hydrogen bonding in the other half is weakened by intramolecular nonbonded steric repulsions. This

Table 1. ^{13}C-NMR assignments for α,β-, α,α- and β,β-dimethylmesobilirubin analogs: **1** (α*S*,β′*S*), **2** (α*R*,β′*S*), **3** (α*S*,α′*S*), **4** (α*R*,α′*S*), **5** (β*S*,β′*S*), and **6** (β*R*,β′*S*) in $CDCl_3$ at 22°C[a]

Position	1	(*P*) 2	(*M*)	3	4	5	6
1,19-CO	174.88 174.91	174.63 174.94	174.07 175.04	174.91	174.89	174.92	174.58 175.02
2,18	123.41 123.89	123.62 123.73	123.96 124.10	123.91	123.92	123.35	123.45
2,18-CH_3	7.93	7.92	7.77	7.95	7.93 7.97	7.95	7.93 7.94
3,17	148.33 148.42	148.19 148.35	147.92 148.30	148.42	148.41	148.39	148.29 148.32
3,17-CH_2CH_3	17.83	17.81		17.86	17.84	17.82	17.84
3,17-CH_2CH_3	14.87	14.87		14.89	14.88	14.90	14.81
4,16	128.18 128.29	128.35 128.38	128.24 128.67	128.27	128.24 128.84	128.25	128.43 128.47
5,15-CH=	100.37 100.51	100.43 100.57	100.17 100.85	100.63	100.64	100.29	100.15 100.55
6,14	123.23 123.27	123.27 123.32	123.20 123.42	123.23	123.20	123.31	123.45
7,13	119.17 122.39	119.31 122.70	117.55 121.66	119.25	119.24	122.42	122.14 122.75
7,13-CH_3	10.25 11.01	9.79 10.17	10.99 11.54	10.27	10.26	11.01	9.72 10.98
8,12	124.18 124.79	123.93 123.95	124.47 124.89	124.14	123.94 124.13	124.84	123.88 124.75
α-CH	39.14	39.18	40.17	39.17	39.14	—	—
α-CH_2	39.53	38.52	39.57	—	—	39.56	38.95 39.65
α-CH_3	19.67	19.24	17.11	19.68	19.18 19.66	—	—
β-CH	26.49	28.07	26.54	—	—	26.47	26.55 28.16
β-CH_2	28.01	27.96	26.00	28.06	28.04 29.70	—	—
β-CH_3	21.00	19.58	20.90	—	—	20.94	19.74 20.82
COOH	179.20 182.29	178.07 182.35	179.20 180.97	182.35	182.34	180.14	178.00 178.07
9,11	132.80 133.27	132.68 133.37	131.90 134.34	133.16	131.92 133.15	132.93	132.73 132.92
10-CH_2	21.98	23.94	22.54	22.17	22.69	21.85	23.80

[a] Values reported for 5×10^{-3} M solutions in ppm downfield from $(CH_3)_4Si$.

makes **4** and **6** more polar than **3** and **5**, less migrating on silica TLC, faster moving on reverse phase HPLC, less soluble in $CHCl_3$, and more partitionable into pH 7.4 buffer from $CHCl_3$.[5]

Like **3** and **5**, **1** is predicted to adopt preferentially the ***M***-helical conformation of Figure 1 because the relevant α and β stereocenters of **1**, **3**, and **5** all have the *S*-configuration. The ^{1}H-NMR signals of **1** are thus doubled – a composite of those in **3** and **5**. In contrast, the ^{1}H-NMR signals of **2** form two sets of double signals, akin to a composite of those in **4** and **6** – as explained above in the ^{13}C-NMR discussion. Again the signals denoted ***P*** are more intense than those denoted ***M***. The ratio of integrals

Table 2. ^{1}H-NMR assignments of α,β-, α,α- and β,β-dimethylmesobilirubins: **1** (α*S*,β′*S*), **2** (α*R*,β′*S*), **3** (α*S*,α′*S*), **4** (α*R*,α′*S*), **5** (β*S*,β′*S*), and **6** (β*R*,β′*S*) in 10^{-3}M $CDCl_3$ solutions at 22°C

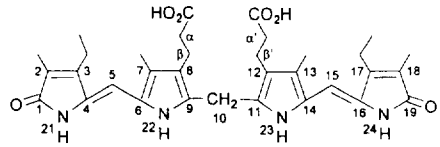

Position	1	2 (*P*)	2 (*M*)	3	4	5	6
α,α′-COO*H*	13.6	13.7	13.8	13.7	13.7	13.6	13.7
21,24-NHCO	10.49 10.73	10.45 10.65	9.97 10.89	10.55	9.84 10.54	10.68	10.23 10.81
22,23-NH	9.04 9.08	8.96 9.29	9.07 9.18	9.09	9.09 9.37	9.04	8.94 9.32
2,18-CH_3	1.86	1.86	1.81	1.86	1.86	1.85	1.85
3,17-C*H*$_2$CH$_3$	2.48[a]	2.48[a]		2.48[a]	2.48[a]	2.48[a]	2.48[a]
3,17-CH$_2$C*H*$_3$	1.12[b]	1.12[b]		1.12[b]	1.12[b]	1.11[b]	1.12[b]
5,15-CH=	6.03 6.05	6.04	5.98	6.05	6.05 6.07	6.04	6.04 6.05
7,13-CH_3	2.15 2.24	2.11 2.15	2.15 2.24	2.15	2.14 2.15	2.24	2.11 2.24
α-CH	3.04[c]	3.03[c]	3.15[c]	3.05[q]	3.03[c] 3.05[c]	—	—
α-CH_2	2.70[d] 3.09[e]	2.70[l] 2.99[m]		—	—	2.70[v] 3.08[w]	2.68, 2.72[v] 2.96, 3.08[z]
α-CH_3	1.45[f]	1.45[f]	1.42[f]	1.45[f]	1.45[f] 1.46[f]	—	—
β-CH	3.45[g]	3.23[n]	3.41[n]	—	—	3.45[x]	3.26[c] 3.44[c]
β-CH_2	2.42[h] 2.90[i]	2.40[o] 2.88[p]		2.42[r] 2.90[s]	2.42[t] 2.90[u]	—	—
β-CH_3	1.34[j]	1.67[j]	1.33[j]	—	—	1.35[y]	1.34[y] 1.65[y]
10-CH_2	3.99[k] 4.11[k]	4.20[k] 4.33[k]	3.98[k] 4.18[k]	4.04	4.04 4.08	4.06	4,17[k] 4.34[k]

[a] q, J=7.6 Hz; [b] t, J=7.6 Hz; [c] AB*X*, m; [d] *A*′B′X′, ^{3}J=2.9, ^{2}J=18.3 Hz; [e] A′*B*′X′, ^{3}J=12.3, ^{2}J=18.3 Hz; [f] d, J=7.1 Hz; [g] A′B′*X*′, ^{3}J=2.9, 12.3, 7.3 Hz; [h] *A*BX, ^{3}J=2.5, ^{2}J=14.1 Hz; [i] AB*X*, ^{3}J=12.1; ^{2}J=14.1 Hz; [j] d, J=7.3 Hz; [k] AB, ^{2}J=15.6 Hz; [l] *A*′B′X′, ^{3}J=4.1, ^{2}J=18.3 Hz; [m] A′*B*′X′, ^{3}J=4.5, ^{2}J=18.3 Hz; [n] A′B′*X*′, m; [o] *A*BX, ^{3}J=2.4, ^{2}J=14.3 Hz; [p] *AB*X, ^{3}J=12.2, ^{2}J=14.3 Hz; [q] AB*X*, ^{3}J=2.2, 12.2, ^{2}J=14.4 Hz; [r] *A*BX, ^{3}J=2.2, ^{2}J=14.4 Hz; [s] A*B*X, ^{3}J=12.2, ^{2}J=14.4 Hz; [t] *AB*X, ^{3}J=2.9, ^{2}J=14.5 Hz; [u] A*B*X, ^{3}J=12.1; ^{2}J=14.5 Hz; [v] *AB*X, ^{3}J=3.0, ^{2}J=18.2 Hz; [w] A*B*X, ^{3}J=12.3, ^{2}J=18.2 Hz; [x] AB*X*, ^{3}J=3.0, 12.3, 7.4 Hz; [y] d, J=7.4 Hz; [z] *A*′B′X′, ^{3}J=4.8, ^{2}J=17.4 Hz.

for lactam NHs (10.65 ppm: 10.89 ppm) or (10.45 ppm: 9.97 ppm) is 78: 22. The same ratio is found for the pyrrole NH pairs, the C(10)-CH_2, and β′-CH_3 signals.

The coupling constants in the propionic acid chains of **1** and **2** provide further insight into the importance of intramolecular hydrogen bonding to pigment conformation. The -C$_\beta$H$_2$-C$_\alpha$H(Me)- and -C$_\beta$H(Me)-C$_\alpha$H$_2$-segments of the propionic acid chains of **1** are found in $CDCl_3$ to exhibit the well-defined ^{1}H-NMR ABX spin system with coupling constants characteristic of the segmental geometry shown in Figure 3A and found in **3** and **5**. In $(CD_3)_2SO$, these segments exhibit averaged

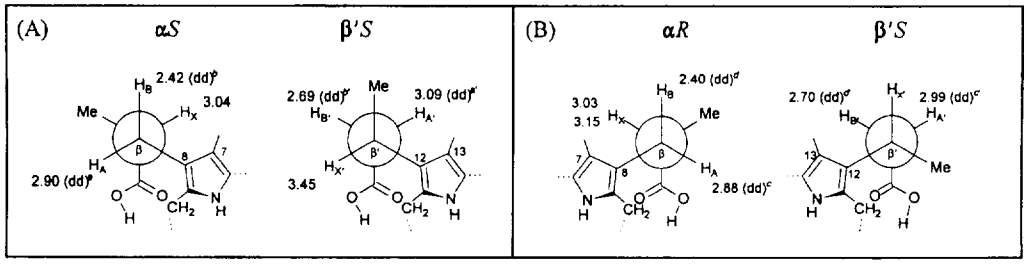

Figure 3. Conformations of the -$C_\beta H_2$-$C_\alpha H$(Me)- and -$C_\beta H$(Me)-$C_\alpha H_2$- segments of the propionic acid groups of (A) **1** and (B) **2** showing the ABX spin systems and coupling constants characteristic of restricted rotation found in the fixed staggered geometry in bilirubin ridge-tile shape (see Figure 1). The ^{1}H-NMR chemical shifts in $CDCl_3$ are shown next to the hydrogens, each H_A and H_B a doublet of doublets and the coupling constants are: [a] $^3J_{AX}$ 12.1, $^2J_{AB}$ 14.1 Hz; [b] $^3J_{BX}$ 2.5, $^2J_{AB}$ 14.1 Hz; [a'] $^3J_{A'X'}$=12.3, $^2J_{A'B'}$ 18.3 Hz; [b'] $^3J_{B'X'}$ 2.9, $^2J_{A'B'}$ 18.3 Hz; [c] $^3J_{AX}$ 12.2 Hz, $^2J_{AB}$ 14.3 Hz; [d] $^3J_{BX}$ 2.4, $^2J_{AB}$ 14.3 Hz; [c'] $^3J_{A'X'}$ 4.3, $^2J_{A'B'}$ 18.3 Hz; [d'] $^3J_{B'X'}$ 4.1, $^2J_{A'B'}$ 18.3 Hz.

coupling constants (6.7 and 7.2 Hz) for an A_2B pattern, characteristic of greater conformational flexibility/motion in the propionic acid groups. Similarly, the -$C_\beta H_2$-$C_\alpha H$(Me)- segment of **2** exhibits a well-defined ABX spin system in $CDCl_3$, again with coupling constants characteristic of the segmental geometry of Figure 3B. Coupling constants from the -$C_\beta H$(Me)-$C_\alpha H_2$- segment was more difficult to determine due to overlapping signals. While the coupling constants $^2J_{AB}$ and $^3J_{AX}$ of an ABX pattern was found, the large ^3J typical of antiperiplanar protons could not be extracted. Here, as in **1**, the coupling constants (6.7 and 7.2 Hz) in $(CD_3)_2SO$, represent averaged values, consistent with greater conformational mobility than in $CDCl_3$. From these important data, we conclude that the propionic acid chains at C(8) in **1** and **2** are held in a similar fixed conformation, as is the propionic acid chain at C(12) in **1** but not in **2**. This would be consistent with predominantly intramolecularly hydrogen-bonded ridge-tile conformations of **1** and **2** in $CDCl_3$ solvent.

Nuclear Overhauser effect

Experimental evidence for folded, monosite or two-site intramolecularly hydrogen bonded conformation of α,β-methylated mesobilirubins **1** and **2** comes from $^1H\{^1H\}$-nuclear Overhauser-effect (NOE) measurements. A quantitative estimate of all observable NOEs in compounds **3** and **5**[5a] was made using a standard steady-state difference NOE experiment.[19] In the most stable ***M***-helical conformation of **3** the pyrrole methyl groups at C(7) and C(13) lie close to the propionic acid α,α′-hydrogens and distant from the α,α′-methyl groups, as confirmed by NOE measurements. Irradiation of C(7)/C(13)-methyl signal at 2.15 ppm gave a 2.6% enhancement on the α,α′-CH signal at 3.05 ppm and vice versa, an 11.1% NOE on the C(7)/C(13)-methyl signal was found by irradiating the α,α′-CH, along with an 0.8% NOE on the C(10)-CH_2. No NOE was found by irradiating the α,α′-methyl signal at 1.45 ppm (except for an NOE on the α,α′-hydrogens), which shows that these methyl groups are located on the periphery of folded conformer of **3**.

In compound **5**, the most stable ***M***-helical conformer brings the C(10)-CH_2 close to propionic acid β,β′-hydrogens and distant from the β,β′-methyl groups with the latter being closer to the C(7), C(13)-pyrrole methyls. Irradiation of the last at 2.24 ppm produced a 1.6% NOE enhancement of the β,β′-methyls at 1.35 ppm and vice versa, irradiating the 1.35 ppm signal gave a 2.6% NOE on the β,β′-methyls. As expected, a stronger NOE related the signals at 3.45 ppm (β,β′-hydrogens) and 4.06 ppm(C(10)-CH_2): 3.7% and 13.6%, respectively. However, irradiation of the C(10)-CH_2 did not show any NOE on the β,β′-methyl groups.

NOEs relating the acid O*H* and lactam N*H* protons indicated strong intramolecular hydrogen bonding in the folded ***M***-helical conformations of **3** and **5**. Irradiation of the CO_2H (13.6 ppm) signals of **3** and **5** gave 6.2% and 4.5% enhancements of the corresponding lactam N*H* signals, respectively. These values are similar to the NOE data reported for mesobilirubin-IXα and bilirubin.[20] The latter

NOE experiments were at 2.11 T; our results were at 7.05 T. The small differences relate to the fact that NOE are magnetic field dependent. At low temperature (−40°C) we found virtually the same NOEs as at room temperature. In addition to the above-mentioned measurements, other strong NOE enhancements found between the lactam N*H* and pyrrole N*H* (20–23%) and between the C(5)/C(15)-vinyl hydrogens and the C(3)/C(17)-CH_2CH_3 and the C(7)/C(13)-CH_3 (3–8%) confirmed that the dipyrrinone moieties of **3** and **5** maintain a nearly planar syn-*Z* conformation. These difference spectra integration data served also for evaluating NOE magnitudes in the experiments described below, but because they are always present in mesobilirubins **1–6** they are not discussed in detail later.

As Table 2 shows, the ^{1}H-NMR spectra of compounds **1, 2, 4**, and **6** are much more complex than those of **3** and **5** due to the presence of two nonidentical dipyrrinone halves, *e.g.*, the C(8)/C(12)-propionic acid side chains constitute an AA′BB′XX′ spin system instead of single ABX found in **3** and **5**. This rendered selective irradiations difficult, and the NOE difference spectra contained more "subtraction artifacts."

Pulsed field gradient NOE spectroscopy

A new method (GOESY) for measuring *transient* NOE enhancements by the use of pulsed field gradients (PFG) was recently proposed.[21] This method avoids computation of *difference* spectra, affording no subtraction artifacts and thus greater confidence in measuring small NOE enhancements. However, the integral enhancement from this new experiment can not be related directly to the percentage enhancement measured from NOE difference spectra. The measurements on rubins **3** and **5** using the PFG NOE experiment qualitatively confirmed the results from the NOE difference spectra. Irradiations of aliphatic region protons (4–1 ppm) gave a more reliable NOE signal. However, irradiation of the acid COO*H* signal did not show an NOE on the lactam N*H* and vice versa. This lack of an NOE might be attributed to an unusually long relaxation time (T_1) of COO*H* protons that is incompatible with the experimental conditions.

The PFG NOE measurement on rubin **1** showed a very strong NOE between the lactam N*H* at 10.73 ppm and the pyrrole N*H* at 9.08 ppm and between the lactam N*H* at 10.49 ppm and pyrrole N*H* at 9.04 ppm, thus pairing the sets in the each dipyrrinone unit. The most important NOEs for describing the 3D structure of **1** were found between the α-CH multiplet (3.03 ppm) and the C(7)-CH_3 at 2.15 ppm, found similarly in **3**, and between the β′-CH multiplet (3.45 ppm) and one of C(10)-CH_2 hydrogens (part of an AB pattern at 3.99 ppm), found similarly in **5**. Excitation of the C(13)-CH_3 (2.24 ppm) gave a moderate NOE on the β′-CH_3 (1.35 ppm). No NOEs were found from irradiation of the α-CH_3 group at 1.46 ppm, except those of propionic chain hydrogens. Using NOE difference spectra and irradiating the acid COO*H* protons gave a 2–4% enhancement of both lactam N*H* signals. Taken collectively, these NOE data strongly support the ***M***-helicity, completely intramolecularly hydrogen-bonded conformation of rubin **1**.

The C_2-symmetrical compounds (**3** and **5**) as well as **1** all exhibited easily detectable NOEs by both difference and PFG methods. However, the NOE experiments on rubins possessing a symmetry plane (**4** and **6**) were not as conclusive. The *meso* compounds **4** and **6** probably have more internal motion and are floppier than **3** and **5**. Spin saturation transfer occurred in these cases, rendering the NOE analysis difficult. For example, excitation of C(7)/C(13)-CH_3 of **4** gave a very weak NOE to the α,α′-CH (3.04 ppm) and to the α,α′-CH_3 (1.45 ppm). Similarly, irradiation of the C(7)/C(13)-CH_3 (2.11 and 2.24 ppm) of **6** gave a weak NOE to the β,β′-CH (3.26 ppm) and to the β,β′-CH_3 (1.34 ppm), respectively. These and similarly doubled NOEs support the view that rubins **4** and **6** exist in helical conformations which allow only one set of completely formed (or tight) triad of intramolecular hydrogen bonds, leaving the second set to form an awkward and looser fit.

In a behavior similar to that found in **4** and **6**, rubin (α*R*,β′*S*)-**2** exhibited relatively weak PFG NOEs. Despite these weak effects, the crucial NOEs pointing to the predominant conformation of **2** were extracted. An observed moderate NOE between the α-CH (3.03 ppm) and C(7)-CH_3 (2.15 ppm) is consistent with a ***P***-helical conformation of **2**. This permits strong intramolecular hydrogen

bonding of the C(8) but not the C(12)-propionic acid chain with the opposing dipyrrinone. Although **2** has the α*R*-configuration, the NOE is similar to that observed for rubin **3**. Currently, the C(8) and not the C(12)-propionic acid chain of **2** controls the dominant ***P***-helicity. A moderate NOE is found between the β′-CH (3.23 ppm) and the C(13)-CH_3 (2.11 ppm), as well as a weak NOE between the β-CH_3 (1.67 ppm) and one of the C(10)-CH_2 protons (4.33 ppm). These NOEs also support the thesis that ***P***-helicity conformation is predominant in **2**, in contrast to **5**, which also has the β*S*-configuration (see the discussion above on **5**).

Conformational analysis

In **1** and **2** the ^{1}H-NMR data clearly indicate a predominance of intramolecularly hydrogen-bonded ridge-tile structures such as those in Figure 1. Intramolecular allosteric nonbonded effects of the methyl groups substituted on the propionic acid side chains of such ridge-tile structures are predicted to displace the conformational equilibrium toward the ***M***-helicity isomer when the stereochemistry at α or β is *S*, and toward the ***P***-helicity isomer when it is *R*.[5,8] A β*S*-methyl induces a nonbonded steric repulsion between the methyl group and C(10)-CH_2- in the ***P***-helicity conformer, but not in the ***M***. Similarly, an α*S*-methyl induces a nonbonded steric repulsion between the methyl group and a C(7) or C(13) ring methyl in the ***P***-helicity conformer but not in the ***M***. Consequently, the ***M***-helicity diastereomer is predicted to be strongly favored over the ***P*** when the relevant stereogenic centers are both *S* (as in **1**). Here, the conformational selection imposed by the *S* stereochemistry at a β-carbon is reinforced by that of the *S* stereochemistry at an α-carbon. Less clear is the prediction when one stereocenter is *S* and the other *R*, as in the α*R*,β′*S* diastereomer (**2**) where the nonbonded steric interactions created by the β′*S* stereochemistry act in opposition to those created by the α*R* stereochemistry. However, the appearance of two sets of ^{1}H- and ^{13}C-NMR signals for **2** in $CDCl_3$ with different intensity indicates the presence of dominant ***P***-helicity conformer which exceeds (overmatches) the ***M***-helicity conformer >3:1. This conclusion is supported also by data from NOE experiments.

Circular dichroism and stereochemistry

The effectiveness of the α and β methyls in displacing the conformational equilibrium of Figure 1 may be detected and analyzed by circular dichroism (CD) spectroscopy. Intense bisignate Cotton effects are seen for the long wavelength transition(s) of **1** and **2** (Figure 4). Previously, it was shown[5] that such CD Cotton effects are also observed for both **3** and **5** in $CHCl_3$. The origin of the observed Cotton effects is not due simply to the introduction of stereogenic centers on the propionic acids because one would expect only a weak, monosignate CD associated with π→π* excitation from a dipyrrinone chromophore perturbed by dissymmetric vicinal action.[17] Rather, the bisignate spectra are characteristic of an exciton system in which two chromophores interact by coupling locally excited π→π* transitions (electric transition dipole coupling).[6,8] The component dipyrrinone chromophores of the bichromophoric rubins have strongly allowed long-wavelength electronic transitions ($\in^{max}_{410}$ ~37,000) and only a small interchromophoric orbital overlap in the folded conformation (Figure 1). They interact through resonance splitting, i.e., by electrostatic interaction of the local transition moment dipoles, which are oriented along the long axis of each dipyrrinone.[8,17] Such intramolecular exciton interaction produces two long wavelength transitions in the UV–vis spectrum and two corresponding bands in the CD spectrum. One band is higher in energy, and one is lower in energy, with the splitting being dependent on the strength and relative orientation of the dipyrrinone electric dipole transition moments. When observed by UV–vis spectroscopy, the two electronic transitions overlap to give the typically broadened and sometimes split long wavelength absorption band found in bilirubins. In the CD spectra, however, where the two exciton transitions are oppositely signed, bisignate spectra are typically seen – as predicted by theory.[8,22]

According to exciton chirality theory,[22] the signed order of the bisignate CD Cotton effects may be used to predict the relative orientation of the two electric dipole transition moments, one from

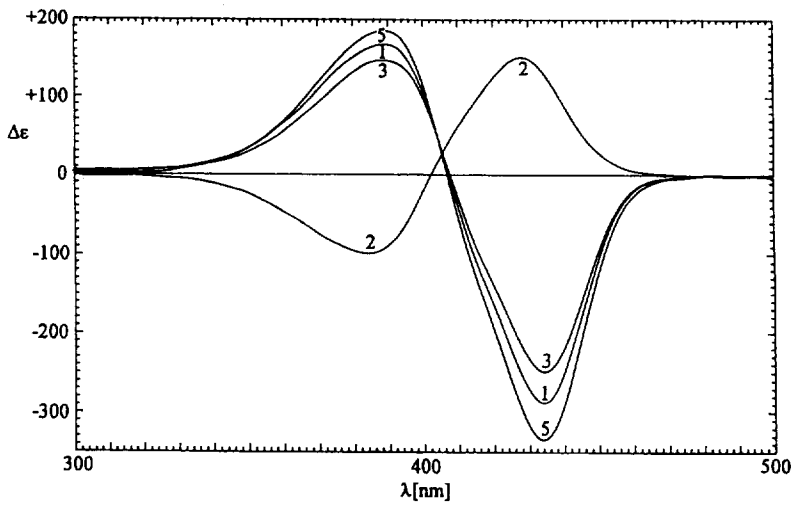

Figure 4. Circular dichroism of 1.5×10^{-5} M solutions of α,β′-dimethylmesobilirubins in chloroform. Spectrum 1: **1** (α*S*,β′*S*), Spectrum 2: **2** (α*R*,β′*S*), Spectrum 3: **3** (α*S*,α′*S*), and Spectrum 5: **5** (β*S*,β′*S*) at 22°C.

each dipyrrinone of the rubin. Thus, a positive exciton chirality (long wavelength positive Cotton effect followed by a negative short wavelength Cotton effect) corresponds to a positive torsion angle between the transition dipoles, and a negative exciton chirality (long wavelength negative Cotton effect followed by a positive short wavelength Cotton effect) corresponds to a negative torsion angle. The ***M***-helicity conformer of Figure 1 is predicted to have a negative exciton chirality; the ***P***-helicity is predicted to have a positive exciton chirality. Therefore, in **1**, **3** and **5** the ***M***-helicity conformer is predicted to dominate the equilibrium, while in **2** the ***P***-helicity conformer is predominant.

Even in a polar protic solvent (CH_3OH) capable of interfering with the intramolecular hydrogen bonding motif of Figure 1, the CD intensities of **1**, **3** and **5** remain quite strong (Figure 5), although the CD intensity of **2** is quite reduced. The Cotton effect signs remain the same as in $CHCl_3$. In all solvents except $(CH_3)_2SO$, **1** exhibits a negative exciton chirality (Table 3), suggesting a predominance of the ***M***-helicity conformer and confirming the predictions drawn above and based on nonbonded intramolecular steric interactions in the α*S*,β′*S* diastereomer. Even in the most polar solvents, the CD spectra of **1**, **3** and **5** remain nearly as strong as those in nonpolar solvents (Table 3), which suggests that it is difficult to disrupt intramolecular hydrogen bonding. The CD intensities of **1** are typically within 80–90% of those seen in **3** and **5**: being more intense than those of **3** and less intense than those of **5**. The data indicate that the conformational equilibrium (Figure 1) for **1** is substantially displaced toward ***M***, that the α*S* and β′*S* methyls act in concert to displace the conformational equilibrium.

The situation differs significantly in the (α*R*,β′*S*) diastereomer **2**, where the α*R* methyl prefers the ***P***-helicity conformer, and the β′*S* methyl prefers the ***M***. In all of the solvents except $(CH_3)_2SO$, **2** exhibits intense *positive* exciton chirality (Table 3), consistent with the equilibrium of Figure 1 being displaced toward the ***P***-helicity conformer. These data suggest that, on balance, the steric influence of the α*R*-methyl counteracts and dominates that of the β′*S*-methyl when they work in opposition (in **2**). Similar dominance of α-methyl over β-methyl is found also in (α*R*,α′*R*,β*S*,β′*S*)-tetramethylmesobilirubin-XIIIα.[23] However, the dominance is not as effective in polar solvents, where the CD intensities of **2** fall to 15–60% of those of **1**. In solvents such as C_2H_5OH and CH_3OH, the Cotton effects are weakest, but in more polar aprotic solvents the Cotton effects of **2** are ~50% of the values in hexane. Although the ***P***-helicity conformer of **2** dominates the conformational equilibrium, it is clear from the conclusion based on NMR that the less intense Cotton effects (relative to **1**) are due to the presence of some ***M***-helicity conformer.

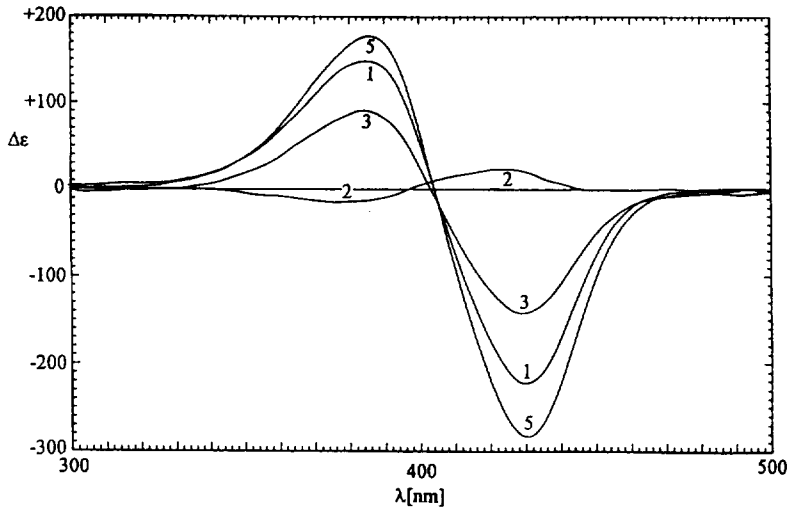

Figure 5. Circular dichroism of 1.5×10^{-5} M solutions of α,β′-dimethylmesobilirubins in methanol. Spectrum 1: **1** (α*S*,β′*S*), Spectrum 2: **2** (α*R*,β′*S*), Spectrum 3: **3** (α*S*,α′*S*), and Spectrum 5: **5** (β*S*,β′*S*) at 22°C.

The solvent $(CH_3)_2SO$ acts in an exceptional way on the spectra. In **1**, **3** and **5** the Cotton effect intensities drop to <10% of the values in *n*-hexane, as they reverse sign – in **1** and in **5**. The CD of **2** also undergoes sign inversion. It seems probable that the favored folded conformation has become somewhat more open (larger θ angle in Figure 1) to accommodate attachment of the solvent molecules.[24] As shown earlier, flattening the ridge-tile leads to a reorientation of the dipyrrinone electric transition dipole moments to near parallelity (and hence to very weak bisignate CEs) and a change in torsion from (−) to (+) without a change in conformational chirality.

Concluding comments

Intramolecular hydrogen bonding, which is characteristic of natural bilirubin and its analogs, is known to be a dominant force in determining their conformation. The current study shows that when the propionic acid residues are substituted with methyl groups at the α and β positions, thus creating stereogenic centers, mesobilirubin-XIIIα is forced by nonbonded steric interactions to adopt either the ***M*** or ***P***-helicity ridge-tile conformation. With α*S*,β′*S* stereocenters, the ***M***-helicity conformer is dominant. However, when the non-bonded interactions operate in conflict, as in the α*R*,β′*S* configuration, a more open ***P***-helicity ridge-tile predominates. In the more open ridge-tile conformation of **2**, the observed exciton chirality CD is weaker and inverted relative to that of the α*S*,β′*S* isomer (**1**).

Experimental

General

All UV–vis spectra were recorded on a Perkin Elmer model 3840 diode array or Cary 219 spectrophotometer, and all circular dichroism (CD) spectra were recorded on a JASCO J-600 instrument. NMR spectra were obtained on a GN-300 or Varian Unity Plus spectrometers operating at 300 MHz and 500 MHz, respectively. $CDCl_3$ solvent (unless otherwise noted) was used and chemical shifts were reported in δ ppm referenced to residual $CHCl_3$ ^1H signal at 7.26 ppm and ^{13}C signal at 77.00 ppm. J-modulated spin-echo experiment (*A*ttached *P*roton *T*est) was used to obtain ^{13}C-NMR spectra. The steady-state NOE enhancements were measured (300 MHz) by difference spectroscopy using 5 sec irradiation time which caused 80–95% saturation of the target signal. The acquisition time was 3.6 sec and the relaxation delay, 10–20 sec. One hundred twenty-eight (128) transients were

Table 3. Comparison of CD and UV–vis spectral data of α,β′-dimethylmesobilirubins-XIIIα at 22°C[a]

Pigment	Solvent	ϵ^b	CD			UV	
			$\Delta\epsilon^{max}(\lambda_1)$	λ_2 at $\Delta\epsilon=0$	$\Delta\epsilon^{max}(\lambda_3)$	ϵ^{max}	λ(nm)
1	Hexane	1.9	+ 166 (389)	403	- 346 (430)	63,800	432
						56,200	411
2			- 98 (384)	400	+ 179 (427)	59,300	428
3			+ 126 (389)	403	- 268 (430)	55,300	434
						48,300	414
5			+ 194 (388)	402	- 423 (430)	60,400	431
						53,600	411
1	CCl_4	2.2	+ 159 (393)	407	- 331 (434)	62,400	436
2			- 91 (390)	405	+ 181 (433)	58,300	434
3			+ 120 (393)	408	- 259 (436)	55,300	438
5			+ 179 (392)	406	- 393 (434)	60,800	435
1	$CHCl_3$	4.7	+ 167 (389)	407	- 288 (434)	58,200	432
2			- 99 (384)	402	+ 151 (428)	56,900	424
3			+ 142 (391)	409	- 251 (436)	56,000	433
5			+ 186 (389)	407	- 337 (434)	55,800	431
1	THF	7.3	+ 159 (388)	406	- 281 (433)	59,200	432
2			- 40 (394)	413	+ 62 (433)	55,000	416
3			+ 123 (390)	407	- 225 (434)	52,000	432
5			+ 188 (390)	406	- 338 (433)	57,900	431
1	$ClCH_2CH_2Cl$	10.4	+ 170 (390)	407	- 281 (433)	58,600	431
2			- 95 (388)	406	+ 160 (432)	58,600	431
3			+130 (390)	408	- 229 (436)	52,000	430
5			+ 193 (389)	407	- 332 (433)	57,100	430
1	$(CH_3)_2CO$	20.7	+ 158 (386)	404	- 269 (430)	58,700	427
2			- 57 (383)	402	+ 92 (426)	56,700	418
3			+ 129 (388)	405	- 230 (431)	55,600	426
5			+ 182 (387)	404	- 322 (430)	57,100	427
1	CH_3CH_2OH	24.3	+ 149 (388)	406	- 230 (433)	58,300	426
2			- 34 (384)	399	+ 52 (426)	57,200	422
3			+ 110 (388)	404	- 170 (431)	58,000	430
5			+ 168 (389)	405	- 284 (434)	57,600	426
1	CH_3OH	32.6	+ 147 (385)	404	- 223 (430)	58,900	425
2			- 15 (376)	397	+ 24 (424)	57,700	422
3			+ 85 (387)	405	- 140 (422)	55,700	426
5			+ 177 (386)	405	- 285 (431)	60,800	425
1	CH_3CN	36.2	+ 155 (384)	403	- 258 (429)	57,300	424
2			- 55 (385)	403	+ 91 (428)	55,200	420
3			+ 124 (387)	404	- 216 (430)	55,200	425
5			+ 181 (384)	403	- 315 (429)	56,700	423
1	$(CH_3)_2SO$	46.5	- 11 (379)	395	+ 15 (425)	60,000	428
2			+ 31 (382)	401	- 25 (425)	62,500	428
3			+ 9 (393)	406	- 18 (428)	52,800	426
5			- 6 (369)	385	+ 23 (425)	56,700	425
1	CH_3NHCHO	182.4	+ 178 (384)	401	- 282 (427)	63,500	427
2			- 51 (384)	400	+ 77 (427)	62,800	427
3			+ 135 (384)	401	- 204 (427)	56,700	428
5			+ 200 (383)	400	- 359 (427)	66,000	426

[a] Conc. ~1.5×10^{-5} M. [b] Dielectric const. from Gordon, A.J., Ford, R.A. *The Chemist's Companion*, Wiley, NY (1972), pp 4-8.

acquired for well degassed 2.5×10^{-3} M $CDCl_3$ solutions interleaving after every 8 scans. The pulsed field gradient transient NOE experiment[21] (500 MHz) used selective 90° pulse of 40 msec and the mixing time was varied around the relevant T1, usually τ_{mix}=0.4 sec. Optical rotations were measured on a Perkin–Elmer model 141 polarimeter. HPLC analyses were carried out on a Perkin–Elmer Series 410 high-pressure liquid chromatograph with a Perkin–Elmer LC-95 UV–vis spectrophotometric detector (set at 420 nm) equipped with a Beckman–Altex ultrasphere IP 5 μm C-18 ODS column (25 × 0.46 cm) kept at 35°C. The flow rate was 1.0 ml.min^{-1}. The mobile phase was 0.1 M di-n-octylamine acetate buffer in 5% aqueous methanol (pH 7.7 at 25°C). Radial chromatography was carried out on

Merck Silica gel PF_{254} with $CaSO_4$ preparative layer grade, using a Chromatotron (Harrison Research, Inc., Palo Alto, CA). Melting points were determined on a Mel-Temp capillary apparatus and are uncorrected. Combustion analyses were carried out by Desert Analytics, Tucson, AZ.

Spectral data were obtained in spectral grade solvents (Aldrich or Fischer). Di-n-octylamine, formic acid, *p*-chloranil (tetrachloro-1,4-benzoquinone), and sodium borohydride were from Aldrich. HPLC grade solvents (Fischer) were dried and distilled prior use: tetrahydrofuran (THF) from $LiAlH_4$, methanol from magnesium methoxide, dimethylsulfoxide from CaH_2, and dichloromethane from P_2O_5.

3,17-Diethyl-8-(2-methoxycarbonyl-2(R,S)-methylethyl)-12-(2-carboxy-1(S)-methylethyl)-2,7,13,18-tetramethyl-(21H,24H)-bilin-1,19-dione (7)

A mixture of 495 mg (1.5 mmol) racemic dipyrrinone **10**,[5b] 474 mg (1.5 mmol) optically pure dipyrrinone **11**,[11] 1.85 g (7.5 mmol) *p*-chloranil, 660 mL of CH_2Cl_2, and 33 mL of formic acid was refluxed for 24 h. The volume was reduced by distillation to one half and the reflux continued for an additional 6 h. Then the mixture was chilled overnight at −20°C. The separated solid was filtered, the blue filtrate was washed with H_2O (3×300 mL), dried (Na_2SO_4), filtered, and the solvent was removed under vacuum. The crude mixture of three verdins (**7**, **8**, **9**) was separated by radial chromatography (4–7% CH_3OH/CH_2Cl_2) collecting the bright blue band with medium polarity. After removing the solvent 382 mg (81%) of pure verdin monomethyl ester **7** was obtained. It had mp 184–193°C; ^{1}H-NMR: δ 1.11 (d, 3H, J=5.8 Hz), 1.17 (d, 3H, J=5.9 Hz), (1.25, 1.26) (2×q, 6H, J=7.4 Hz), 1.84 (s, 3H), 1.86 (s, 3H), 2.14 (s, 6H), 2.57 (m, 8H), 2.97 (m, 1H), 3.23 (m, 1H), (3.52, 3.62) (2×s, 3H), (5.98, 5.99) (2×s, 1H), (6.14, 6.15) (2×s, 1H), (6.72, 6.76) (2×s, 1H), 8.45 (br.s, 1H), 9.69 (br.s, 1H) ppm; ^{13}C-NMR: δ 8.10, 8.26, 9.41, 9.47, 10.84, 14.50, 16.68, 16.93, 17.84, 17.95, 20.59, 20.62, 27.76, 27.78, 28.45, 28.59, 39.75, 40.91, 41.41, 51.69, 51.76, 96.61, 98.29, 114.41, 114.63, 126.80, 126.82, 127.58, 128.37, 128.66, 128.74, 134.10, 137.82, 141.23, 141.29, 144.78, 144.82, 146.71, 147.91, 147.97, 171.73, 171.75, 175.31, 175.34, 176.14, 176.63 ppm.

Dimethylmesobilirubins 1 and 2

A mixture of 314 mg (0.5 mmol) verdin **7**, 150 mL of THF:CH_3OH=1:1, 150 mL of 0.2 M aqueous NaOH, and 160 mg ascorbic acid was purged with N_2 and stirred under N_2 at 50°C for 4 h. After cooling the mixture was diluted with 100 mL of 0.1 M aq. NaOH and washed with $CHCl_3$ (2×50 mL) which was discarded. The aqueous layer was acidified with 10% HCl and the product extracted with $CHCl_3$ (5×50 mL). The combined extracts were washed with H_2O (2×100 mL), dried (Na_2SO_4), filtered, and the solvent was removed under vacuum to afford mesobiliverdin diacids used immediately in the next step.

The verdin diacids from above were dissolved in 80 mL of dry deoxygenated THF, cooled with ice bath and 1.90 g (50 mmol) $NaBH_4$ was added, followed by 40 mL of dry methanol over 10 min. After 5 min. more stirring, the mixture was diluted with 300 mL of H_2O and acidified with CH_3COOH. The product was extracted with $CHCl_3$ (4×100 mL), washed with H_2O (3×100 mL), dried (Na_2SO_4), filtered, and the solvent was evaporated under vacuum. The crude mixture was separated by radial chromatography (1–2% CH_3OH/CH_2Cl_2) and after evaporation of the corresponding pure fractions they were recrystallized from $CHCl_3/CH_3OH$ to afford:

(−)-8-(2-Carboxy-2(S)-methylethyl)-12-(2-carboxy-1(S)-methylethyl)-3,17-diethyl-2,7,13,18-tetramethyl-(10H,21H,23H,24H)-bilin-1,19-dione (1)

The less polar diastereomer **1**, 122 mg (40% yield), was obtained as bright yellow crystals with (R_f 0.83) on silica gel TLC (2% CH_3OH in CH_2Cl_2). It had mp 281–284°C (decomp.) and $[\alpha]_D^{20}$ 5530 (c 4.5×10^{-3}, $CHCl_3$). ^{1}H-NMR $(CD_3)_2SO$: δ 0.88 (d, 3H, J=6.7 Hz), 0.94 (d, 3H, J=7.1 Hz), 1.08 (t, 6H, J=7.5 Hz), 1.77 (s, 6H), 1.99 (s, 3H), 2.09 (s, 3H), 2.17 (m, 1H, *A*BX), 2.20 (q, 1H, J=7.1 Hz), (2.32, 2.37) (2×1H, *A'B'*X', ^{3}J=7.7, 8.0; ^{2}J=15.2 Hz), 2.48 (q, 4H, J=7.5 Hz), 2.53 (m, 1H, A*B*X),

3.10 (q, 1H, J=7.4 Hz), (3.94, 4.00) (2H, AB, ^{2}J=16.7 Hz), 5.94 (s, 1H), 5.95 (s, 1H), 9.80 (s, 1H), 9.85 (s, 1H), 10.19 (s, 1H), 10.22 (s, 1H), 11.90 (br.s, 2H) ppm; ^{13}C-NMR $(CD_3)_2SO$: δ 8.07, 9.49, 10.52, 14.84, 16.71, 17.17, 19.76, 24.03, 26.94, 27.71, 39.92, 40.33, 97.46, 97.97, 118.26, 121.70, 121.93, 122.37, 122.89, 122.95, 123.10, 123.36, 127.76, 128.03, 129.63, 131.20, 147.24 147.29, 172.02, 173.70, 177.42 ppm. *Anal.* Calcd. for $C_{35}H_{44}N_4O_6$(616.7): C, 68.16; H, 7.19; N, 9.08. Found: C, 67.57; H, 7.07; N, 8.67.

*(+)-8-(2-Carboxy-2(*R*)-methylethyl)-12-(2-carboxy-1(*S*)-methylethyl)-3,17-diethyl-2,7,13,18-tetramethyl-(10*H*,21*H*, 23*H*,24*H*)-bilin-1,19-dione (2)*

This pigment was crystallized to give 113 mg (37%) as a bright yellow more polar (R_f 0.24) on silica gel TLC (2% CH_3OH in CH_2Cl_2) diastereomer. It had mp 288–292°C (decomp.); $[\alpha]_D^{20}$ +2370 (*c* 4.8×10^{-3}, $CHCl_3$); ^{1}H-NMR $(CD_3)_2SO$: δ 0.88 (d, 3H, J=6.8 Hz), 0.94 (d, 3H, J=7.1 Hz), 1.08 (t, 6H, J=7.5 Hz), 1.77 (s, 6H), 1.98 (s, 3H), 2.06 (1H, *A*BX, ^{3}J=7.3, ^{2}J=15.0 Hz), 2.09 (s, 3H), 2.20 (q, 1H, J=7.1 Hz), 2.32 (2H, *A′B′*X′, J=7.2, 6.7 Hz), 2.43 (m, 1H, A*B*X), 2.51 (q, 4H, J=7.5 Hz), 3.08 (q, 1H, J=7.2 Hz), (3.90, 4.04) (2H, AB, ^{2}J=16.8 Hz), 5.94 (s, 1H), 5.95 (s, 1H), 9.83 (s, 1H), 9.87 (s, 1H), 10.22 (s, 1H), 10.25 (s, 1H), 11.90 (br.s, 2H) ppm; ^{13}C-NMR $(CD_3)_2SO$: δ 8.04, 9.45, 10.54, 14.81, 16.89, 17.14, 19.67, 24.02, 26.89, 27.73, 39.86, 40.20, 97.39, 97.92, 118.33, 121.69, 121.83, 122.32, 122.83, 122.89, 123.12, 123.35, 127.66, 127.92, 129.67, 131.12, 147.20, 147.26, 171.99, 173.64, 177.39 ppm. *Anal.* Calcd. for $C_{35}H_{44}N_4O_6$(616.7): C, 68.16; H, 7.19; N, 9.08. Found: C, 68.02; H, 7.19; N, 8.88.

Acknowledgements

We thank the National Institutes of Health (HD 17779) for generous support of this work and the National Science Foundation (CHE-9214294) for assistance in purchasing the 500 MHz NMR spectrometer used in this work. We thank Prof. A.J. Shaka (UC Irvine) for sending us his PFG NOE pulse sequence and Mr Lew Cary for invaluable assistance in obtaining NOE data from it. S.E. Boiadjiev is on leave from the Institute of Organic Chemistry, Bulgarian Academy of Sciences, Sofia.

References

1. Chowdury, J.R.; Wolkoff, A.W.; Chowdury, N.R.; Arias, I.M. In *The Metabolic and Molecular Bases of Inherited Disease*, Scriver, C.R.; Beaudet, A.L.; Sly, W.S.; Valle, D., eds., 1995, Vol. II, 2161–2208.
2. McDonagh, A.F. In *The Porphyrins*; Dolphin, D., ed.; Academic Press: New York, **1979**, *6*, 293–491.
3. Blauer, G; Wagnière, G. *J. Am. Chem. Soc.* **1975**, *97*, 1949–1954.
4. Pu, Y-M.; McDonagh, A.F.; Lightner, D.A. *J. Am. Chem. Soc.* **1993**, *115*, 377–380.
5. (a) Boiadjiev, S.E.; Person, R.V.; Puzicha, G.; Knobler, C.; Maverick, E.; Trueblood, K.N.; Lightner, D.A. *J. Am. Chem. Soc.* **1992**, *114*, 10123–10133. (b) Puzicha, G.; Pu, Y-M.; Lightner, D.A. *J. Am. Chem. Soc.* **1991**, *113*, 3583–3592.
6. Lightner, D.A.; Gawroński, J.K.; Wijekoon, W.M.D. *J. Am. Chem. Soc.* **1987**, *109*, 6354–6362.
7. (a) Navon, G; Frank, S.; Kaplan, D. *J. Chem. Soc. Perkin Trans. 2* **1984**, 1145–1149. (b) Kaplan, D.; Navon, G. *Isr. J. Chem.* **1983**, *23*, 177–186.
8. Person, R.V.; Peterson, B.R.; Lightner, D.A. *J. Am. Chem. Soc.* **1994**, *116*, 42–59.
9. McDonagh, A.F.; Lightner, D.A. *Pediatrics* **1985**, *75*, 443–455.
10. Lightner, D.A.; Wijekoon, W.M.D.; Zhang, M.H. *J. Biol. Chem.* **1988**, *263*, 16669–16676.
11. Boiadjiev, S.E.; Anstine, D.T.; Lightner, D.A. *J. Am. Chem. Soc.* **1995**, *117*, 8727–8736.
12. (a) Shrout, D.P.; Puzicha, G.; Lightner, D.A. *Synthesis* **1992**, 328–332. (b) Boiadjiev, S.E.; Lightner, D.A. *SYNLETT.* **1994**, 777–785.
13. For leading references, see: Falk, H. *The Chemistry of Linear Oligopyrroles and Bile Pigments*; Springer Verlag: NY, **1989**.

14. Trull, F.R.; Rodríguez, M.; Lightner, D.A. *Synthetic Comm.* **1993**, *23*, 2771–2783.
15. McDonagh, A.F.; Assisi, F. *J. Chem. Soc. Chem. Comm.* **1972**, 117–118.
16. (a) Trull, F.R.; Ma, J.S.; Landen, G.L.; Lightner, D.A. *Israel J. Chem.* **1983**, *23 (2)*, 211–218. (b) Lightner, D.A.; Trull, F.R. *Spectroscopy Lett.* **1983**, *16*, 785–803. (c) Lightner, D.A.; Ma, J-S. *Spectroscopy Lett.* **1984**, *17*, 317–327.
17. Boiadjiev, S.E.; Anstine, D.T.; Maverick, E.; Lightner, D.A. *Tetrahedron: Asymmetry* **1995**, *6*, 2253–2270.
18. Nogales, D.F.; Ma, J-S.; Lightner, D.A. *Tetrahedron* **1993**, *49*, 2361–2372.
19. (a) Neuhaus, D.; Williamson, M.P. *The Nuclear Overhauser Effect in Structural and Conformational Analysis*; Verlag Chemie: New York, **1989**. (b) Sanders, J.K.M.; Mersh, J.D. *Prog. Nucl. Magn. Reson.* **1982**, *15*, 353–400.
20. Kaplan, D.; Navon, G. *J. Chem. Soc. Perkin Trans. 2*, **1981**, 1374–1383.
21. (a) Stonehouse, J.; Adell, P.; Keeler, J.; Shaka, A.J. *J. Am. Chem. Soc.* **1994**, *116*, 6037–6038. (b) Stott, K.; Stonehouse, J.; Keeler, J.; Hwang, T.-L.; Shaka, A.J. *J. Am. Chem. Soc.* **1995**, *117*, 4199–4200.
22. Harada, N.; Nakanishi, K. *Circular Dichroic Spectroscopy – Exciton Coupling in Organic Stereochemistry*; University Science Books: Mill Valley, CA, 1983.
23. Boiadjiev, S.E.; Lightner, D.A. *Tetrahedron: Asymmetry* **1996**, *7*, 1309–1322.
24. (a) Gawroński, J.K.; Poonski, T.; Lightner, D.A. *Tetrahedron* **1990**, *46*, 8053–8066. (b) Trull, F.R.; Shrout, D.P.; Lightner, D.A. *Tetrahedron* **1992**, *48*, 8189–8198.

(Received in USA 3 April 1997; accepted 5 May 1997)